CHAPTER 1

Introduction

Practical implementation of fiber optic sensors for structural health monitoring provides crucial economic benefits regarding lower life-cycle costs of the civil infrastructure systems. Application of sensor technologies for early damage detection and prognosis leads directly to a reduction of maintenance, repair and insurance expanses. The well-established distributed fiber optic sensing methods based on scattering effects in silica fibers offer decisive advantages such as real-time remote monitoring over kilometer-long distances, operational reliability of sensors in an electromagnetic environment as well as two-dimensional sensor design using smart geosynthetics for monitoring of large geotechnical structures like dikes, railways, tunnels or embankments.

Stimulated Brillouin scattering (SBS) in silica optical fibers has been intensively studied for several decades [1–3]. The acquired knowledge has been successfully applied in fields of signal processing [4], THz signal generation [5], phase conjugation [6], lasing [7, 8] and optical storage [9]. Applications for distributed strain and temperature sensing based on SBS in silica optical fibers were investigated intensively [10, 11]. In all SBS sensors the Brillouin frequency shift (BFS) depends on temperature and strain. State of the art SBS sensing setups are capable of monitoring fiber lengths beyond 100 km with a few meter spatial resolution [12–14] and down to extremely short ranges with spatial resolutions ranging from centimeter [15] to millimeter [16] and micrometer [17].

Fiber optic sensors are not limited to SBS and are covering numerous fields of impacts for example temperature [18], strain [11], humidity [19–23], radiation [24, 25], vibration [26], acoustics [27–29], refractive index of liquids, partial discharge in power cable joints and terminations [30], velocity of sound outside a sensing fiber [31], subsurface seismic monitoring [32], concentrations of salts in liquid compounds [33].

Compared to silica optical fibers, perfluorinated graded-index polymer optical fibers (PFGI-POFs) offer higher break down strain up to 100 % [34], minimal bending radii below 2 mm, higher sensitivity to temperature and lower sensitivity to strain [35]. These beneficial characteristics make the commercially available PFGI-POF potentiality interesting for

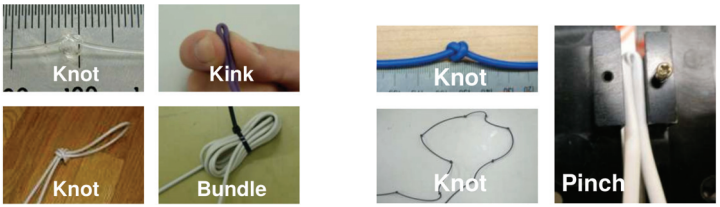

Figure 1.1: Demonstration of PFGI-POFs being knotted, bundled and pinched with and without fiber jacketing. Reprinted from `http://www.lucina.jp/eg_fontex/pdf/Tecnhical.pdf`

embedded fiber sensor applications silica fibers can not reach and withstand. Figure 1.1 underlines the fiber's flexibility under extreme mechanical influences.

Polymer optical fibers (POFs) have been employed in several areas of applications such as short-range data communication [36], polymer optical fiber amplifier [37], radiation monitoring [38], clinical monitoring of patients [39–41], cell and bacteria detection in clinical probes [42, 43], illumination [44] and humidity sensing [23].

In PFGI-POFs spontaneous [45, 46] and stimulated [47] Brillouin scattering was observed almost a decade ago. Distributed Brillouin sensing was intensively studied in the last years [48–50] and the latest results reported on spatial resolutions in the centimeter-scale with high repetition rates [51]. However, all presented distributed Brillouin fiber sensors in PFGI-POF are limited to a few tens of meters due to a high attenuation at 1550 nm ($\approx$ 250 dB/km [52]). Aiming to reduce the sensor fibers propagation loss, an alternative wavelength of 1319 nm was chosen as suggested in [18, 46]. As demonstrated in [46] Nd:YAG lasers at this wavelength are well suited to generate SBS in PFGI-POF due to a lower fiber attenuation ($\leq$ 37 dB/km at 30 °C [22]). The aim of this thesis is to design and implement a distributed Brillouin sensor based on BOFDA for PFGI-POFs. The adopted BOFDA scheme is demonstrated in a laboratory setup to achieve a sensing range of 86 m with 3.4 m spatial resolution. Furthermore, the impact of humidity changes on the Brillouin gain spectrum were empirically investigated for the first time.

This thesis deals with the advancement and implementation of distributed Brillouin sensing in PFGI-POF. A theoretical view at physical basics of Brillouin scattering is given in chapter 2. Chapter 3 introduces the light propagation in PFGI-POF and provides a comprehensive view on SBS in graded-index multimode fibers. The requirements for an reliable interconnection between PFGI-POFs and silica fibers to generate SBS are presented in chapter 4. The three major concepts of distributed Brillouin sensing are summarized in chapter 5 with special emphases on the frequency-domain approach and on distributed Brillouin sensors in PFGI-POFs. The entire relationships between SBS parameters and the environmental parameters strain, temperature and humidity are thoroughly presented in chapter 6, respectively. Chapter 7 discusses the influence of amplitude noise on the measurement accuracy of Brillouin sensors. Finally, the laboratory setup along with experimental results is laid out in chapter 8.

CHAPTER 2

Brillouin scattering in optical fibers

In general, Brillouin scattering refers to the inelastic interaction of an incident optical wave with material waves in a medium. Léon Brillouin theoretically predicted the spontaneous light scattering on thermally excited acoustic waves in 1922 [53]. In 1930 the experimental confirmation of spontaneous Brillouin scattering in liquids was given by Gross [54]. Stimulated Brillouin scattering was first observed in 1964 after the invention of the laser [55]. In the 1970s the development of low-loss glass fibers [56] resulted in intense research on optical transmission systems [57]. Brillouin scattering in optical fibers and the threshold of its stimulated process were investigated as SBS is a significant factor limiting the maximum transmittable power in optical communication systems [58, 59]. On the other hand, since then Brillouin scattering in optical fibers has been employed in various applications like high resolution spectroscopy [60], quasi-light storage and optical delay [4, 9], signal generation and processing [5, 6], sensing [10, 11], viscosity determination of liquids [61], microscopic imaging [62] and characterization of elastic properties in geosciences [63].

2.1 Spontaneous and stimulated Brillouin scattering

Light scattering is a result of inhomogeneities of the refractive index in a medium. Almost all propagation media have static fluctuations of the local dielectric permittivity causing elastic scattering of light in all directions. Thermally excited lattice vibrations in optical fibers already result in density fluctuations, which spread with the velocity of sound v_a. The scattering of light on these thermally excited acoustic waves in a medium is called spontaneous Brillouin scattering (SpBS). Due to the photoelastic effect, the sound waves induce a periodic modulation of the refractive index of the medium. The reflection and diffraction of light on (quasi)-stationary periodic gratings of refraction index changes is known as Bragg reflection [1]. The wavelength of the acoustic wave λ_a describes the spatial period of the refractive index modulation. When Braggs condition is satisfied, a wave with a vacuum wavelength of λ_P is reflected at such a periodic refractive index lattice. Equation 2.1 gives Braggs condition, where n_P is the group index of the medium for the

incident pump wave and θ the angle between incident and reflected wave propagation direction. Figure 2.1 schematically illustrates the Bragg reflection.

$$\lambda_P = 2n_P\lambda_a sin\frac{\theta}{2} \tag{2.1}$$

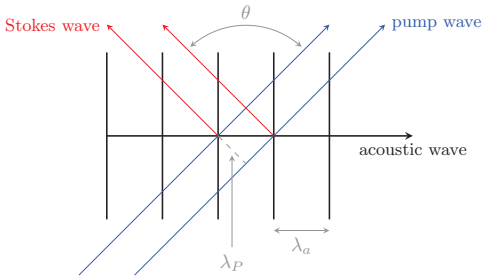

Figure 2.1: Reflection of light on an acoustic wave. Partial reflections of the pump wave will superimpose constructively to a scattered Stokes wave if the path difference between each partial reflection is equal to λ_P.

Due to the fact that the refractive index lattice is traveling in the medium with the velocity of sound and the optical pump wave with c/n_P, the Doppler effect has to be considered for the scattered light:

$$f_S = f_P\left(1 - 2n\frac{v_a}{c}sin\frac{\theta}{2}\right) = f_P - f_B(\theta) \tag{2.2}$$

$$f_{AS} = f_P\left(1 + 2n\frac{v_a}{c}sin\frac{\theta}{2}\right) = f_P + f_B(\theta) \tag{2.3}$$

When the acoustic wave moves away from the pump wave, a Stokes wave with smaller frequency f_S is generated and an anti-Stokes wave of greater frequency is generated when the sound wave travels towards the pump wave. The maximum frequency offset can be observed when $\theta = \pi$ and refers to the counter propagation of the pump and Stokes wave. This maximum frequency offset is known as the material-specific Brillouin frequency shift or in short Brillouin frequency shift (BFS). In case of $\theta = \pi$ follows, that the Brillouin frequency shift f_B is equal to the acoustic frequency f_a in Eqn. 2.1.

$$f_B = 2n_P\frac{v_a}{c}f_P \tag{2.4}$$

Spontaneous Brillouin scattering on thermally excited sound waves occurs in optical fibers. For single mode fibers (SMFs) sensing systems based on SpBS have been presented [48, 64, 65]. However, due to arbitrary thermal motions, the SpBS propagation directions are arbitrary, too. Thus, SpBS has no dominant direction of propagation in an optically and acoustically multi-modal propagating medium and the scattered light intensity is very weak.

If the intensity of the pump wave exceeds a certain threshold at which the power transfer to the Stokes wave is higher than the attenuation it will experience, a stimulated process can occur. A small portion of SpBS Stokes waves is exactly counter propagating to the pump wave with a frequency f_S and amplified due to the Brillouin gain (see section 2.2). This process is called stimulated-amplified spontaneous Brillouin scattering, which limits the maximum transmittable power in an optical fiber. The Brillouin threshold needed to start this process will be closer described in section 2.3.

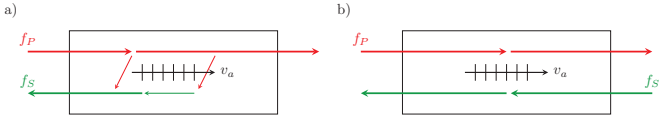

Figure 2.2: Stimulated Brillouin scattering process initiated by a) spontaneous Brillouin scattering and b) two counter propagating optical waves.

Alternately, two counter propagating optical waves at a frequency of $f_S = f_P - f_B$ can initiate stimulated Brillouin scattering (SBS) as illustrated in Fig. 2.2. The interference between the Stokes and pump waves result in an optical beating. The envelop frequency of the beating is equal to the difference frequency of both optical waves. The beating moves in the same direction as the pump wave due to the conservation of energy and momentum in the quantum mechanical model. Due to electrostriction, the intensity modulation of the beating is transfered into a density modulation of the medium. Electrostriction is associated with the property of dielectric materials and is caused by molecules which move or relocate in presence of an electric field. The density modulation of the medium is characterized by periodical variations, which associate to an acoustic wave within the medium. Consequently to the density modulations, the refractive index demonstrates the same modulations, which leads to a periodic grating in the medium fulfilling Eqn. 2.1. By increasing the pump power, the optical beating also increases, which results in raised grating structures in the medium and consequently to an exponential increment of backscattered Stokes wave power. The Stokes wave accumulates the scattered pump power along the interaction length and is therefore amplified [3]. If an optical wave at the frequency of $f_{AS} = f_P + f_B$ is injected to the counter propagating pump wave, the direction of energy flow remains as described in the process above. Thus, along the interaction length the anti-Stokes wave is attenuated depending on the pump power.

The boundary condition for optical waves is given by the Helmholtz equation [1]:

$$\nabla^2 \mathbf{E} + n^2(f)\frac{f^2}{4\pi^2 c^2}\mathbf{E} = 0 \tag{2.5}$$

Nonlinear effects in optical fibers are a result of either an intensity dependence of the refractive index or a scattering phenomena. In case of intense electromagnetic fields a homogeneous material can behave like a nonlinear medium. Consequently, the material polarization $\mathbf{P}$ is no longer proportional to the electric field $\mathbf{E}$ and can be described by a Taylor series [2]:

$$\mathbf{P} = \varepsilon_0 \chi^{(1)}\mathbf{E} + \varepsilon_0 \chi^{(2)}\mathbf{E}^2 + \varepsilon_0 \chi^{(3)}\mathbf{E}^3 + \cdots = \mathbf{P}^L + \mathbf{P}^{NL} \tag{2.6}$$

where $\chi^{(i)}$ denotes the k-th order susceptibility and ε_0 the permittivity in vacuum. The linear susceptibility $\chi^{(1)}$ contributes dominantly to $\mathbf{P}$. The second order susceptibility $\chi^{(2)}$ causes second harmonics and sum-frequency generation. However, for media with symmetric molecule structures, like silica, $\chi^{(2)}$ vanishes. Therefore, silica optical fibers do not exhibit second order nonlinear refractive effects [66]. As written earlier, the electrostriction follows the nonlinear polarization due to a change of susceptibility and is expressed by [2]:

$$\mathbf{P}_i^{NL} = \Delta\varepsilon \mathbf{E}_i(\mathbf{r},t) = \frac{\gamma_e}{\rho_0}\Delta\rho \mathbf{E}_i(\mathbf{r},t). \tag{2.7}$$

$\Delta\varepsilon$ represents the change of dielectric permittivity, γ_e the electrostrictive coefficient, ρ_0 the average density of the guiding material and $\Delta\rho$ the function of the density wave in the guiding medium. Classically, the SBS is expressed by the interaction of a pump wave $\mathbf{E}_P$, a Stokes wave $\mathbf{E}_P$ and an acoustic wave $\Delta\rho$. In the following theoretical process only optical single-mode systems are considered with one acoustic wave co-propagating with the pump wave and oscillating in its own direction of propagation. The theory of optical and acoustical multi-mode systems will be discussed further in chapter 3.

$$\begin{aligned}
\mathbf{E}_P &= \mathbf{e}_P \frac{1}{2} E_P(z,t)\ exp\{j(2\pi f_P t - k_P z)\} + c.c. \\
\mathbf{E}_S &= \mathbf{e}_S \frac{1}{2} E_S(z,t)\ exp\{j(2\pi f_S t + k_S z)\} + c.c. \\
\Delta\rho &= \frac{1}{2} A(z,t)\ exp\{j(2\pi f_B - k_B z)\} + c.c.
\end{aligned} \tag{2.8}$$

where $\mathbf{e}_i = \mathbf{E}_i/|\mathbf{E}_i|$ are normalized polarization vectors. The temporal and spatial propagation of Eqn. 2.8 in an electrostrictive, isotropic and homogeneous medium is described as follows [67]:

$$\begin{aligned}
\nabla^2\mathbf{E}_P - \frac{n^2}{c^2}\frac{\partial^2\mathbf{E}_P}{\partial^2 t^2} &= \mu_0 \frac{\partial^2 \mathbf{P}_P^{NL}}{\partial^2 t^2} \\
\nabla^2\mathbf{E}_S + \frac{n^2}{c^2}\frac{\partial^2\mathbf{E}_S}{\partial^2 t^2} &= \mu_0 \frac{\partial^2 \mathbf{P}_S^{NL}}{\partial^2 t^2} \\
v_a^2\nabla^2(\Delta\rho) - \frac{\partial^2\Delta\rho}{\partial^2 t^2} - \Gamma\frac{\partial\Delta\rho}{\partial t} &= \nabla\cdot\mathbf{F}
\end{aligned} \tag{2.9}$$

where Γ is the acoustic damping coefficient, $\mathbf{P}_i^{NL}$ are the nonlinear polarization fields of Eqn. 2.7 and $\Delta\rho$ represents the density variations. All equations are coupled through the electrostrictive force F. This electrostrictive force is expressed using material constitutive relations [2]:

$$\nabla\cdot\mathbf{F} = -\frac{\gamma_e}{2}\nabla^2\langle E^2\rangle \tag{2.10}$$

Thus, the nonlinear polarization fields for the pump and probe wave follow as:

$$\begin{aligned}
\mathbf{P}_P^{NL} &= \mathbf{e}_P \frac{1}{2}\frac{\gamma_e}{\rho_0} A(z,t) E_S(z,t)\ exp\{j(2\pi f_P t - k_P z)\} + c.c. \\
\mathbf{P}_S^{NL} &= \mathbf{e}_S \frac{1}{2}\frac{\gamma_e}{\rho_0} A^*(z,t) E_P(z,t)\ exp\{j(2\pi f_S t + k_S z)\} + c.c.
\end{aligned} \tag{2.11}$$

In case $\mathbf{P}^{NL} = 0$, the two optical waves from Eqn. 2.9 are not interacting and their powers remain constant. Therefore, their propagation is expressed by simple plain waves. If $\mathbf{P}^{NL} \neq 0$, the fields $\mathbf{E}_P$ and $\mathbf{E}_S$ are linked via the nonlinear polarization. In most cases the effect of nonlinear polarization is modest compared to the linear polarization for only a few optical wavelengths. Hence, linear solutions for the wave fields can be applied and include the slowly varying envelope approximation of [68]. Under the named assumptions the system of differential coupled equations simplifies to a set of scalar equations [67]:

$$\begin{aligned}
\frac{\partial}{\partial z}E_P - \frac{n}{c}\frac{\partial}{\partial t}E_P + \frac{\alpha}{2}E_P &= -j\frac{k_S\gamma_e}{4\varepsilon\rho_0}AE_S \\
-\frac{\partial}{\partial z}E_S + \frac{n}{c}\frac{\partial}{\partial t}E_S - \frac{\alpha}{2}E_S &= -j\frac{k_S\gamma_e}{4\varepsilon\rho_0}A^*E_P \\
\frac{\partial}{\partial z}A + \frac{2\pi f_B - j\Gamma k_B^2}{2\pi f_B v_a}\frac{\partial}{\partial t}A &= -(\mathbf{e}_P\cdot\mathbf{e}_S)j\frac{k_B\gamma_e}{4v_a^2}E_PE_S^*
\end{aligned} \tag{2.12}$$

α is the optical loss of the guiding medium. During the entire interaction process, the energy and momentum have to be conserved. Therefore, the frequencies and wave vectors of all three waves are related by:

$$\begin{aligned}
f_B &= f_P - f_S \\
\mathbf{k}_B &= \mathbf{k}_P - \mathbf{k}_S
\end{aligned} \tag{2.13}$$

where f_B is the frequency and k_B the wave vector of the acoustic field. According to the system of equations in (2.12), static and dynamic SBS processes are covered. For continuous wave signals ($\partial/\partial t = 0$), steady-state conditions for the acoustic field can be considered, which leads to an extinction of the time derivate term. In contrast to the low optical loss for the pump and probe wave, the acoustic wave is attenuated rapidly. In silica the free path of the phonons are usually very short ($\approx 10^{-6}$ m). Hence, the amplitude of the acoustic wave is expressed by [2]:

$$A = j\frac{k_B\gamma_e}{2v_a\Delta f_B}(\mathbf{e}_P\cdot\mathbf{e}_S)E_PE_S^* \tag{2.14}$$

where $\Delta f_B = \Gamma k_B^2$ is the bandwidth of the Brillouin scattering. One observes, that the Brillouin linewidth is directly scaling with the acoustic damping coefficient, which represents the average lifetime of a phonon within the guiding medium [1]. Eventually, inserting Eqn. 2.14 into Eqn. 2.12 delivers two coupled equations, describing the relation between pump and Stokes wave in the SBS process:

$$\begin{aligned}
\frac{\partial}{\partial z}E_P &= -(\mathbf{e}_P\cdot\mathbf{e}_S)\frac{k_Bk_P\gamma_e^2}{8\varepsilon\rho_0v_a\Delta f_B}\,\frac{E_P|E_S|^2}{1-j(2\Delta\nu/\Delta f_B)} - \frac{\alpha}{2}E_P \\
-\frac{\partial}{\partial z}E_S &= -(\mathbf{e}_P\cdot\mathbf{e}_S)\frac{k_Bk_S\gamma_e^2}{8\varepsilon\rho_0v_a\Delta f_B}\,\frac{E_S|E_P|^2}{1-j(2\Delta\nu/\Delta f_B)} - \frac{\alpha}{2}E_S
\end{aligned} \tag{2.15}$$

where $\Delta\nu$ represents the detuning frequency ($\nu - f_B$) between a current frequency state ν and the Brillouin frequency shift given in Eqn. 2.1. The real parts of Eqn. 2.15 cause an energy transfer and consequently an optical gain or an optical loss. Whereas the imaginary parts lead to a nonlinear phase shift. Considering steady state conditions for continuous

pump and probe waves, the equations can be further simplified as the lifetime of the acoustic wave is negligibly small compared to the lifetime of the pump wave. Furthermore, the introduction of optical intensities $I_i = \frac{1}{2} n \varepsilon_0 c |E_i|^2$ for pump and Stokes wave enables Eqn. 2.15 to be written as [1, 3]:

$$\begin{aligned} \frac{\partial I_P}{\partial z} &= -g_B(\Delta\nu) I_P I_S - \alpha I_P \\ \frac{\partial I_S}{\partial z} &= -g_B(\Delta\nu) I_P I_S + \alpha I_P. \end{aligned} \tag{2.16}$$

The new parameter g_B is introduced to describe the Brillouin gain coefficient and its dependency of frequency detuning. The loss resonance f_{AS} caused by SBS is mathematically given in the same manner as for the Stokes scattering. Only the sign of the Brillouin gain coefficient is changed and $f_{AS} > f_P$. The spectral response of the Brillouin loss is equal to its gain as illustrated in Fig. 2.3.

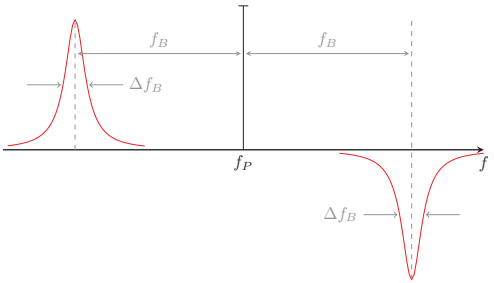

Figure 2.3: Schematic illustration of the Brillouin gain and loss resonances with respect to the pump wave.

Assuming the pump wave power is not exceeding the Brillouin threshold to cause stimulated-amplified spontaneous Brillouin scattering, the intensity of the pump wave is only affected by the attenuation of the medium [3]:

$$I_P(z) = I_P(z = 0)\ exp\{-\alpha z\} \tag{2.17}$$

where z is introduced as a spatial parameter along the guiding medium. $z = 0$ refers to the beginning of the medium at which the pump wave is launched. $z = L$ to the end of the medium at which the Stokes wave is launched. The total length of the medium is L. Thus, the pump intensity at the position L is:

$$I_P(z = L) = I_P(z = 0) \int_0^L exp\{-\alpha z\}\, dz = \frac{I_P(z = 0)}{\alpha} (1 - exp\{-\alpha L\}) = I_P(z = 0) L_{eff}. \tag{2.18}$$

L_{eff} represents the effective length of the medium. It is note, that the SBS does not only depend on intensities but also on the interaction length at which the power density remains sufficiently high [3]. The attenuation of the guiding medium and the total fiber length are

relevant factors to describe the effective length of nonlinear interaction. Consequently, the Stokes wave in Eqn. 2.16 can be written as:

$$\frac{\partial I_S}{\partial z} = I_S\left(-g_B I_P(z) + \alpha\right) \tag{2.19}$$

Combining Eqn. 2.19 and 2.18 gives the intensity of the Stokes wave at the Position $z = L$:

$$I_S(z = L) = I_S(z = 0)\ exp\left\{\frac{-g_B P_P(z = 0) L_{eff}}{A_{eff} + \alpha L}\right\}. \tag{2.20}$$

Hence, the intensity of the Stokes wave at the beginning of the medium is [58]:

$$I_S(z = 0) = I_S(z = L)\ exp\left\{\frac{g_B P_P(z = 0) L_{eff}}{A_{eff} - \alpha L}\right\}. \tag{2.21}$$

Note, that the intensity of the pump wave is given as the ratio of power P_P and effective illuminated area in the medium A_{eff}. Therefore, next to the intensities of the optical waves and the length of optical interaction also the effective illuminated area inside the medium influences affects the SBS process [1–3]. Furthermore, for pump and Stokes wave powers above the Brillouin threshold Eqn. 2.21 is not valid and does not consider the polarization dependence between pump and Stokes wave during the SBS process.

2.2 The Brillouin gain spectrum

The Brillouin gain coefficent $g_B(\Delta\nu)$ and its spectral distribution is approximated by a Lorentzian function. This approximation originates from the acoustic wave in the SBS process as it can be considered a force and damped oscillation [1, 2].

$$g_B(\Delta\nu) = g_p \frac{(\Delta f_B/2)^2}{(\Delta\nu)^2 + (\Delta f_B/2)^2} \tag{2.22}$$

where g_P refers to the peak value of the Brillouin gain coefficient. Its definition was indirectly given in Eqn. 2.15 [2]:

$$g_p = \frac{\eta_P 2\pi n^7 p_{12}^2}{c\lambda_P^2 \rho v_a \Delta f_B} \tag{2.23}$$

with λ_P denoting the pump wavelength and p_{12} referring to the longitudinal elasto-optic coefficient. η_P indicates a dependency on the polarization of the SBS interaction. For optical fibers the state of polarization is not constant due to local birefringence that statistically varies along the fiber in strength and orientation [66]. Thus, the inference of pump and stokes wave causing the beating signal in an optical fiber is dependent on the state of polarization between pump and Stokes wave to each other. η_P represents the polarization mixing efficiency of the pump and Stokes wave given by $\eta_P = |\mathbf{e}_P \cdot \mathbf{e}_S|^2$. Furthermore, a strong dependency on the refractive index with a power to 7 underlines the influence of material properties. A normalized gain distribution of the Brillouin gain spectrum (BGS) is plotted in Fig. 2.4. As mentioned earlier, the amplification of the

Stokes wave comes with a nonlinear phase change. Thanks to the Kramers-Kronig relation, the real and imaginary parts of the susceptibility of a medium are connected and links the absorption coefficient to the refractive index in a dispersive medium. The normalized imaginary part of the Brillouin gain, which corresponds to the phase change during the SBS amplification, is plotted in Fig. 2.4, too.

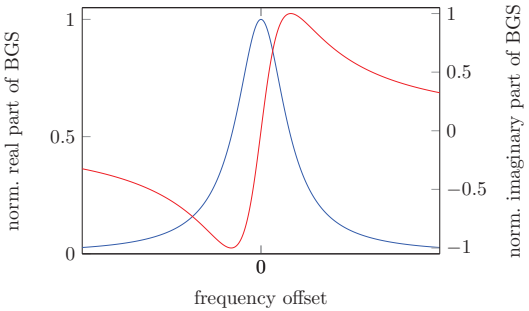

Figure 2.4: Normalized Brillouin gain spectrum splited in real and imaginary part.

However, if pump pulses are temporally shorter than the phonon life time or the linewidth of the pump source, the corresponding pump pulse spectrum is broader than the intrinsic Brillouin linewidth. Consequently, the resulting Brillouin gain spectrum is deformed and Eqn. 2.23 is need to be enhanced to [3]:

$$g_p = \frac{\eta_P 2\pi n^7 p_{12}^2}{c\lambda_P^2 \rho v_a \Delta f_B} \left(\frac{\Delta f_B}{\Delta f_B * \Delta f_P} \right) \tag{2.24}$$

where Δf_P denotes the linewidth of the pump source and $*$ the convolution operation. In case $\Delta f_P \ll \Delta f_B$ the effect of the pump source is negligibly small and the Brillouin linewidth is rather affected by material properties. Thus, narrow linewidth laser sources are in preferential use for the evaluation of a Brillouin gain spectrum.

Among the Brilllouin gain coefficient and the Brillouin linewidth, the Brillouin frequency shift characterizes the gain spectrum. Eqn. 2.4 denotes the dependencies of the frequency shift by the refractive index, the wavelength of the pump wave and the velocity of sound within the medium. The presented derivation of the SBS process assumed one acoustic wave propagating along the direction of the pump wave. In optical fibers this acoustic wave corresponds to a longitudinal wave oscillating in a radial direction [1, 58]. Thus, the velocity of sound for this specific mode in cylindrical media is expressed by $v_a = \sqrt{\epsilon/\rho_0}$, where ϵ is the elastic modulus and ρ_0 the average density of the guiding medium [1]. Consequently, Eqn. 2.4 enhances to:

$$f_B = \frac{2n\ v_a}{\lambda_P} = \frac{2n\sqrt{\epsilon/\rho_0}}{\lambda_P} \tag{2.25}$$